Green Chemistry

PAPER

View Article Online
View Journal

Cite this: DOI: 10.1039/c5gc02548f

Conversion of methoxy and hydroxyl functionalities of phenolic monomers over zeolites†

Rajeeva Thilakaratne,[a,b] Jean-Philippe Tessonnier[b,c] and Robert C. Brown*[a,b,c]

Received 23rd October 2015,
Accepted 10th December 2015

DOI: 10.1039/c5gc02548f

www.rsc.org/greenchem

This study investigates the mechanisms of gas phase anisole and phenol conversion over zeolite catalyst. These monomers contain methoxy and hydroxyl groups, the predominant functionalities of the phenolic products of lignin pyrolysis. The proposed reaction mechanisms for anisole and phenol are distinct, with significant differences in product distributions. The anisole mechanism involves methenium ions in the conversion of phenol and alkylating aromatics inside zeolite pores. Phenol converts primarily to benzene and naphthalene *via* a ring opening reaction promoted by hydroxyl radicals. The phenol mechanism sheds insights on how reactive bi-radicals generated from fragmented phenol aromatic rings (identified as dominant coke precursors) cyclize rapidly to produce polyaromatic hydrocarbons (PAHs). Resulting coke yields were significantly higher for phenol than anisole (56.4% *vs.* 36.4%) while carbon yields of aromatic hydrocarbons were lower (29.0% *vs.* 58.4%). Water enhances formation of hydrogen and hydroxyl radicals, thus promoting phenol conversion and product hydrogenation. From this finding we propose phenol–water–zeolite combination to be a high temperature hydrolysis system that can be used to generate both hydrogen and hydroxyl radicals useful for other kinds of reactions.

1. Introduction

Zeolites are widely used as catalysts to refine crude petroleum to hydrocarbon fuels. They are also recognized for their ability to convert carbohydrate-derived compounds from biomass into aromatic hydrocarbons during pyrolysis.[1–8] ZSM-5 zeolite was reported to be the best in achieving high conversions to aromatic hydrocarbons, mainly due to its unique structure and acid sites.[1,9]

Despite already having an aromatic structure, lignin in biomass presents a unique challenge to upgrading *via* pyrolysis. This is mainly due to the recalcitrant bonds formed from repolymerizing phenolic intermediates produced from lignin during pyrolysis conversion.[10–12] Processes with high ionic energies such as that occur during catalytic process are required to deconstruct and deoxygenate these condensed bonds formed from lignin.[13,14] However, the literature reports poor yields of hydrocarbons for pyrolysis of lignin and upgrading lignin derived bio-oil in the presence of zeolites with high coke (carbonaceous material produced on the surface of the catalyst) generation cited as the reason for this inferior performance.[13,14]

Catalytic pyrolysis of biomass over zeolites is generally considered to occur in two steps: (1) depolymerization and devolatilization; and (2) catalytic conversion of volatiles to hydrocarbons.[15,16] Depolymerization produces phenolic monomers containing hydroxyl, methoxy, carbonyl, vinyl and methyl functionalities and these are abundant in bio-oil obtained from fast pyrolysis of biomass.[10] Of these, hydroxyl and methoxy functionalities are most commonly produced from lignin and are thought to be the driving force of the reactivity of lignin and lignin-derived products.[17] In this study we analyze catalytic upgrading of anisole and phenol using ZSM-5 zeolites to understand the conversion of lignin-derived phenolic monomers with the aim of reducing coke generation and increasing the yield of aromatic hydrocarbons.

Zhu *et al.*[18] describe high temperature non-catalytic decomposition of phenol to its keto-isomers while Friderichsen *et al.*[19] explain how polyaromatic hydrocarbons (PAHs) are formed from anisole. Nowakowska *et al.*[20] studied the kinetics of pyrolysis and oxidation of anisole, mainly focusing on combustion intermediates of lignin and reaction rates. Rahimpour *et al.*[21] discuss anisole conversion in a plasma reactor for catalytic and non-catalytic reactions, but do not provide a mechanistic explanation for these steps. Prasomsri *et al.*[22] explored the effectiveness of anisole conversion in the presence of hydrocarbons during catalytic pyrolysis over HY and HZSM5 zeolite catalyst, although the mechanism of conversion was

[a]Department of Mechanical Engineering, Iowa State University, Ames, IA 50011, USA. E-mail: rcbrown3@iastate.edu
[b]Bioeconomy Institute, Iowa State University, Ames, IA 50011, USA
[c]Department of Chemical and Biological Engineering, Iowa State University, Ames, IA 50011, USA

†Electronic supplementary information (ESI) available. See DOI: 10.1039/c5gc02548f

not explored. Several researcher claim conversion involves a "carbon pool" within the zeolite pores without providing a detailed explanation of the phenomenon.[4,6] Guisnet and Gilson[1] claim that the conversion of high molecular weight hydrocarbons over zeolites occurs *via* the carbonium ions, but provide no details on how oxygenated compounds convert inside zeolite pores. The present study explores the radical and ionic mechanisms involved in the conversion of anisole and phenol monomers over zeolites to produce hydrocarbons.

2. Experimental section

2.1. Material

ZSM-5 zeolite catalyst powder (CBV 2314) in ammonia form with Si/Al mole ratio of 23 and surface area of 425 $m^2\ g^{-1}$ was purchased from Zeolyst International. The catalyst was heated at 5 °C min^{-1} and calcined at 550 °C for 5 hours in a muffle furnace prior to use. The powder was then pressed into pellets using a hydraulic press (Carver, hydraulic unit, USA). The pellets were crushed to form catalysts particles in the size range of 212–300 μm. All reactants including ^{13}C carbon labeled anisole and phenol used in this analysis to validate mechanisms were purchased from Sigma Aldrich with nearly 100% purity (anisole: 99%, phenol: 99%, 1,2,3-trimethoxybenzene: 98%, benzaldehyde: 99%, 1,4-benzoquinone: 98%, hydroquinone: 99%, catechol: 99%, anisole-phenyl-$^{13}C_6$: 99% and 99 atom%, phenol-1-^{13}C: 98% and 99 atom%).

2.2. Methods

A Frontier Tandem system with a micro-pyrolysis reactor and an *ex situ* catalyst bed (Fig. 1) was used for catalytic pyrolysis experiments.[6–8] Liquid monomer in the amount of 250 μg ± 25 μg was placed in a deactivated stainless steel sample cup containing a small disc made of ultra clean, high quality fine glass fibers (Frontier, Auto-Rx disc). This disc adsorbs the monomers to prevent evaporation during the preparation step. The catalyst bed was loaded with 40 mg of prepared zeolite catalyst, which was deemed in preliminary experiments to be sufficient quantity for thorough contacting of the pyrolysis vapors with the zeolite. The monomers were pyrolyzed at 600 °C and the volatiles generated were transported through the catalyst bed, also maintained at 600 °C. This temperature is high enough to provide sufficient activation energy for reaction but low enough to prevent excessive formation of non-condensable gases.[13,14] Volatiles were identified by the GC/MSD and quantified using GC/FID. Gases were identified by injecting known gases and quantified by injecting known gas mixture volumes *via* GC/TCD. After duplicate runs, the coked catalyst bed was analyzed for carbon content using an elemental analyzer (vario MICRO cube, Elementar, USA). Pyrolytic char (carbonaceous material produced in non-catalytic thermal conditions) content was calculated using residue mass in the sample cup after pyrolysis, assuming 100% carbon in the char. A similar procedure was adopted for anisole and phenol carbon isotopes runs used for mechanisms validation purpose.

Non-catalytic pyrolysis runs were also performed for anisole and phenol using similar reaction conditions, without catalyst in the second reactor bed. Influence of water in phenol conversion was analyzed in an identical setup with a catalyst bed, by injecting 0.5 μL, 1 μL and 5 μL quantities of water in to the sample cup, which consist of 250 μg ± 25 μg of phenol and an adsorber disc prior to being pyrolyzed.

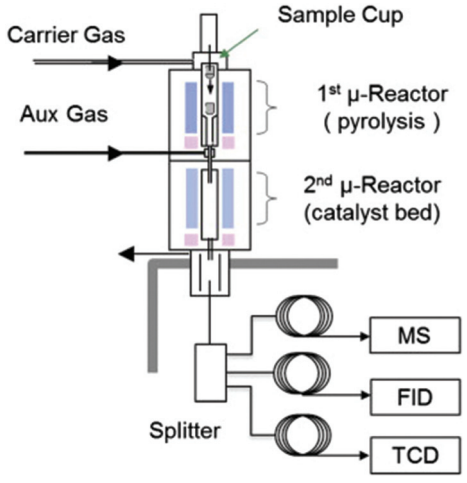

Fig. 1 Schematic diagram of the micro-pyrolysis system used in this study.

3. Results and discussion

As shown in Table 1 anisole produced significantly higher carbon yield of aromatic hydrocarbons (58.4% carbon) than phenol (29.0% carbon), which gives evidence that the type of oxygen functionality attached to the aromatic ring plays an important role in conversion over zeolites. Phenol produced significantly higher coke (56.4% carbon) than anisole (36.4% carbon). Phenol also produced a considerable amount of char (12.4% carbon) from non-catalytic polymerization in the cup. PAHs yield was 17.7% for phenol with only 13.4% for anisole. Most importantly, the selectivity of PAHs for phenol was 61.3% with only 22.9% for anisole. Contrary to the reported role of anisole promoting PAHs, these results indicated that the contribution from phenol for PAHs generation was significantly higher compared to anisole.[19] Gas yields were relatively small and similar for both cases.

Product selectivity was significantly different for these two monomers, as illustrated in Table 1. The main products from anisole were benzene and toluene, while from phenol they were benzene, naphthalene, and biphenyl. This indicates distinct mechanisms for their conversion over ZSM5 catalyst. Even though zeolites provide ionic influence to the reactions, predominantly radical-based mechanisms have been proposed for the catalytic conversion of these two monomers after investigating product formation routes, as explained later.[11,23]

Table 1 Product distribution for catalytic conversion of anisole and phenol (*ex situ* catalysis, pyrolysis temperature = 600 °C, catalyst bed temperature = 600 °C, reactant loading = 0.25 mg, catalyst CBV 2314, catalyst loading = 40 mg)

Feedstock	Anisole	Phenol
Overall yield (%)		
CO	1.1 ± 0.1	1.0 ± 0.1
CO_2	0.3 ± 0.1	0.2 ± 0.1
Catalytic coke	36.4 ± 0.8	56.4 ± 2.5
Pyrolytic char	0.0 ± 0.0	12.4 ± 0.1
Aromatics	58.4 ± 0.7	29.0 ± 1.2
Olefins	2.8 ± 0.2	2.8 ± 0.2
Total	99.1 ± 0.2	101.9 ± 3.8
Aromatics selectivity (%)		
Benzene	47.9 ± 0.5	34.2 ± 0.8
Toluene	21.9 ± 0.0	2.2 ± 0.2
C8 aromatics[a]	4.1 ± 0.0	0.4 ± 0.1
Naphthalene	9.5 ± 0.3	27.9 ± 0.6
Biphenyl	1.2 ± 0.1	11.7 ± 0.0
C9 aromatics[b]	3.2 ± 0.3	2.1 ± 0.1
C10+ aromatics[c]	12.2 ± 0.3	21.7 ± 0.3
Olefin selectivity (%)		
Ethylene	55.1 ± 1.4	46.1 ± 1.8
Propylene	12.4 ± 2.0	23.0 ± 2.8

[a] C8 aromatics including xylenes and ethylbenzene. [b] C9 aromatics include indene and alkylbenzenes. [c] C10+ aromatics include alkylated naphthalenes and higher polyaromatic hydrocarbons (PAHs).

As proposed in this study, anisole conversion starts by producing phenol and methenium ion with the help of acid sites on the surface of the zeolite catalyst (Fig. 2). The methylene radical generated from anisole is thought to be stabilized in the form of methenium ion. Phenol then reacts with the methenium ion to form benzaldehyde with a dehydrogenation step. Next, benzaldehyde decarbonylates to benzene on the acid sites. Supporting these observations, Pramosri *et al.*[22] report phenol as the major intermediate generated from anisole over zeolites. Kim *et al.*[11] show that during fast pyrolysis methoxy functionality converts to a less extent to aldehyde functionality, as described above. The ionic influences of zeolites are expected to enhance this conversion significantly.

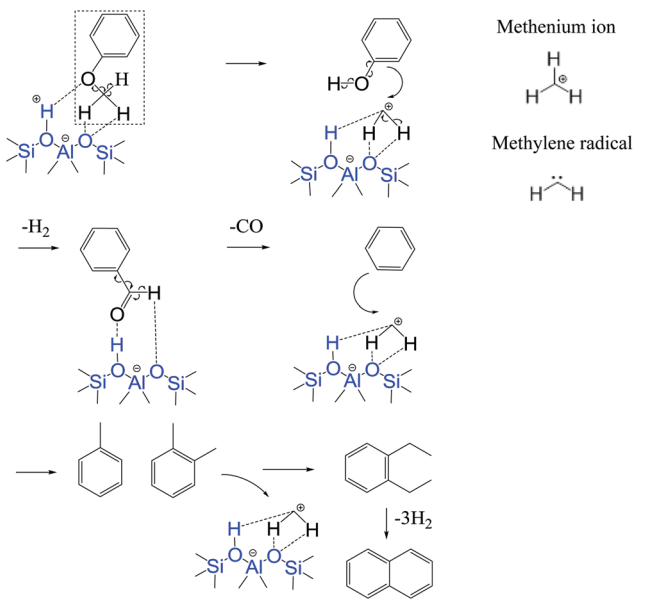

Fig. 2 Proposed mechanism for conversion of anisole over zeolites at 600 °C (line 1: phenol and methenium ion formation, line 2: benzaldehyde decarbonylation, line 3: benzene alkylation in zeolites using methenium ions).

Next, methenium ion acts as an alkylating agent and reacts with benzene to produce toluene, xylenes and a small amount of naphthalenes as final products. These type of electrophilic aromatic substitution reactions under acidic conditions, such as in Friedel–Craft benzene alkylation, are commonly reported in the literature.[24,25] It is also important to note that the production of methenium ions is not sufficient to completely convert phenol to benzene. The remainder of the phenol converts to additional naphthalene and benzene, as subsequently described. A similar pathway exists for conversion of cresol (the other major intermediate of anisole as shown in Fig. S1†) to toluene although not illustrated in Fig. 2.

As shown in Fig. 3 phenol conversion is initiated by generation over the zeolite catalyst of aryl, phenoxy, hydroxyl and hydrogen radicals. Some of these recombine to produce products such as benzene, biphenyl, hydrogen and water. Although previous evidence for this mechanism was not found in the literature, we subsequently present experimental evidence in support of it. From here, the hydroxyl radicals combine with phenoxy radicals to form 1,4-benzoquinone as the major product intermediate. Rapport *et al.*[26] describe the formation of 1,4-benzoquinone from phenol under oxidative conditions *via* a dehydrogenation step. Similarly, dehydrogenation could explain 1,4-benzoquinone formation observed in our study. 1,4-Benzoquinone then goes through ring opening defragmentation *via* cyclopenta-2,4-dien-1-one, eluting carbon monoxide and producing short lived biradicals that rapidly cyclize inside zeolite pores to form benzene, naphthalene and PAHs, as shown in Fig. 3. Existence of these C_2H_2 and C_4H_4 biradicals has not been established in the literature; however, these might be in equilibrium with acetylene and cyclobutadiene (or cumulene), respectively, or exist as surface intermediates.[27] This idea is supported by several previous studies that describe benzene formation starting from acetylene and converting *via* C_2H_2 and C_4H_4 radical intermediates, even at very mild reaction conditions.[28–30]

As illustrated in Fig. 3, higher coke yield observed for phenol could be attributed to the tendency of ring fragmentation bi-radicals to cyclize to higher molecular weight PAHs. The higher ethylene selectivity for anisole could be a result of two methylene radicals combining, whereas higher propylene selectivity for phenol might result from aromatic ring defragmentation, as previously described. Although CO and CO2 can undergo secondary reactions such as water–gas shift and Boudouard reactions, their carbon yields are insufficient to explain mechanisms proposed in this study.[31] The greater energy

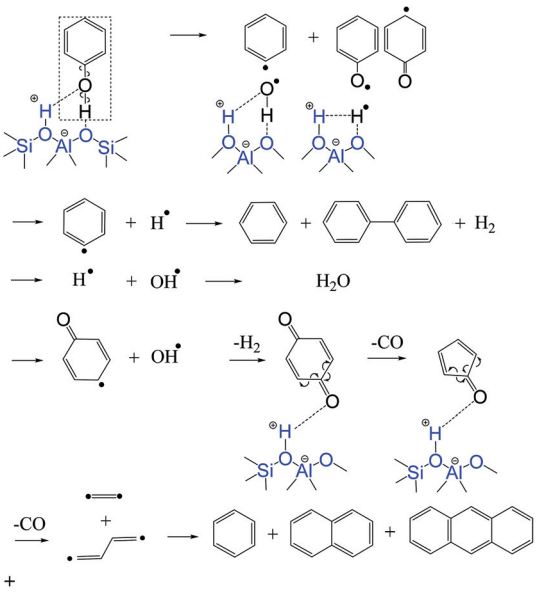

Fig. 3 Proposed mechanisms for conversion of phenol over zeolites at 600 °C (line 1: aryl, phenoxy, hydroxyl and hydrogen radicals formation, line 2 & 3: aryl, hydroxyl and hydrogen radicals recombination, line 4: 1,4-benzoquinone and cyclopenta-2,4-dien-1-one formation and ring fragmentation by decarbonylation, line 5: benzene, naphthalene and PAHs formation).

barrier associated with hydroxyl radical generation and high molecular coke formation can be attributed to lower conversion associated with phenol, while methenium ion assisted intermediate phenol conversion could explain the significantly higher conversion for anisole.[32]

3.1. Validation of the proposed mechanism for anisole and phenol conversion over zeolites

3.1.1. Proposed anisole conversion mechanism. At 600 °C, typical of fast pyrolysis, anisole shows very little decomposition, resulting in small amounts of phenol, benzaldehyde and cresols. According to the mechanism (Fig. 2), anisole in the presence of zeolite catalyst first decomposes to phenol through the action of the surface acid sites. Because phenol has a smaller effective diameter, its kinetic hindrance through the zeolite pores would be reduced compared to anisole.[26,33] As shown in Fig. S1 (see ESI†), anisole reacted over a coked catalyst bed (generated from five consecutive runs of 2 mg anisole over the catalyst) produces phenol as the major oxygenated intermediate. As catalysts fouled with coke have limited internal pore acidity and restricted access, this observation provides evidence that anisole initially convert to phenol over external surface acid sites while subsequent phenol conversion to aromatic hydrocarbons occurs mainly inside pores.[25,26]

The step from phenol to benzene was experimentally validated by co-reacting phenol with 1,2,3-trimethoxybenzene (1 : 1 weight ratio), which is expected to generate methylene radicals that subsequently produce methenium ions over zeolites.[34] The net effect on benzene generation is shown in Table 2 and Fig. 4. When phenol was co-reacted with 1,2,3-trimethoxybenzene, benzene selectivity increased to 40.6%, compared to 34.2% for phenol alone and 36.4% for 1,2,3-trimethoxybenzene alone. Fig. 4 shows that the carbon conversion for benzene in the phenol-1,2,3-trimethoxybenzene combination is 20.3%, significantly higher than theoretical carbon conversion as calculated from individual conversion percentages (15.2%). These observations show that phenol uses methenium ions produced from 1,2,3-trimethoxybenzene for benzene generation in a similar way as the anisole mechanism. The dramatic reduction of toluene selectivity (Table 2) for phenol and 1,2,3-trimethoxy benzene mixture, could be mainly due to the effect of phenol having very low selectivity for toluene. In addition, methylene radicals that contribute to toluene generation for 1,2,3-trimethoxybenzene could be used up for phenol conversion to benzene, reducing toluene in the products for this mixture.

3.1.2. Proposed phenol conversion mechanism. In phenol conversion, formation of biphenyl is evidence for the presence of aryl and hydroxyl radicals. A very high amount of symmetric biphenyl formation is seen as strong evidence of the radical reactions rather than ionic reactions. The presence of water in the MSD chromatograph for phenol (Fig. S2 in ESI†) suggests the generation of hydrogen radicals during the reaction, assuming that hydroxyl radicals are generated as described above. Presences of hydrogen radicals imply the presence of

Table 2 Product selectivity for catalytic conversion of anisole intermediates and 1,2,3-trimethoxybenzene methylene donor (*ex situ* catalysis, pyrolysis temperature = 600 °C, catalyst bed temperature = 600 °C, catalyst CBV 2314, catalyst loading = 40 mg)

Feedstock	Phenol	1,2,3-Trimethoxybenzene	Phenol + 1,2,3-trimethoxybenzene[a]	Benzaldehyde
Benzene	34.2 ± 0.8	36.4 ± 0.6	40.6 ± 0.5	95.5 ± 0.6
Toluene	2.2 ± 0.2	27.0 ± 0.0	13.0 ± 1.1	1.6 ± 0.4
C8 aromatics[b]	0.4 ± 0.1	5.9 ± 0.1	1.6 ± 0.1	0.6 ± 0.2
Naphthalene	27.9 ± 0.6	13.4 ± 0.1	20.2 ± 0.3	0.8 ± 0.1
Biphenyl	11.7 ± 0.0	0.4 ± 0.0	3.2 ± 0.5	0.7 ± 0.2
C9 aromatics[c]	2.1 ± 0.1	3.4 ± 0.1	2.4 ± 0.5	0.2 ± 0.1
C10+ aromatics[d]	21.7 ± 0.3	13.9 ± 0.5	22.1 ± 1.5	0.7 ± 0.1

[a] Sample contains approximately 500 μg of phenol and 1,2,3-trimethoxybenzene mixture at 1 : 1 weight ratio. [b] C8 aromatics including xylenes and ethylbenzene. [c] C9 aromatics include indene and alkybenzenes. [d] C10+ aromatics include alkylated naphthalenes and higher polyaromatic hydrocarbons (PAHs).

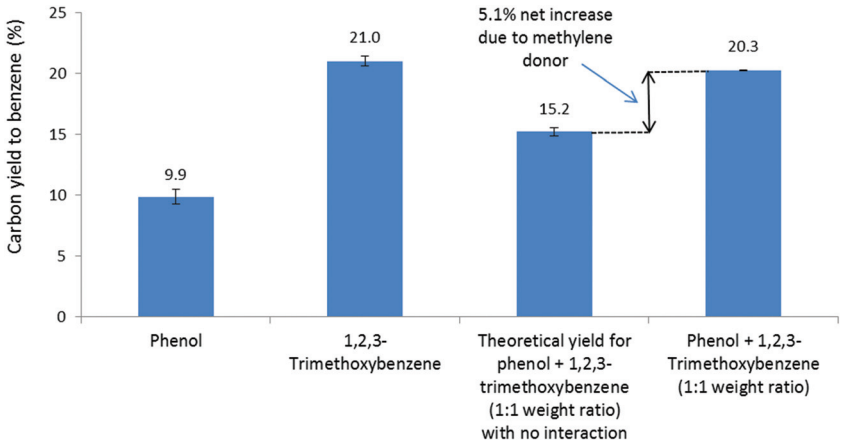

Fig. 4 Comparative analysis of carbon yield of benzene from catalytic conversion of phenol alone and in the presence of a methylene donor (1,2,3-trimethoxybenzene).

phenoxy radicals.[32] Radical recombination is expected to produce benzene and hydrogen as reported for catalytic pyrolysis reactions over zeolites.[1]

Major ring opening step for phenol would be *via* 1,4-benzoquinone. This reaction is bi-molecular as phenoxy radical uses a hydroxyl radical from a different phenol molecule.[26] Resonance of the phenoxy radical can also generate 1,2-benzoquinone isomer similar to 1,4-benzoquinone generation (Fig. 3) but zeolite pore hindrance would favor linear 1,4-benzoquinone as reported in other studies.[33] However it was not possible to experimentally observe 1,4-benzoquinone, which possibly converted inside zeolite pores. To validate this reaction step, 1,4-benzoquinone was reacted with zeolite under identical conditions. In this reaction, 1,4-benzoquinone generated a similar product distribution as phenol, producing mostly benzenes and naphthalene. Hydroquinone, corresponding phenolic derivative of 1,4-benzoquinone, also generate similar product distribution as phenol providing high product selectivity to benzene and naphthalene (Table 3). This implies that hydroquinone and phenol both go through the same intermediate 1,4-benzoquinone. However, 1,4-benzoquinone provide lower C10+ aromatics selectivity mainly due to lack of biphenyl and fluorene produced compared to phenol. Surprisingly, catechol (Table 3) produces significantly different product distribution than phenol mostly with hydrogenated monoaromatics, suggesting a conversion route close to a proposed secondary phenol ring opening mechanism (Fig. S3 in ESI†).

3.1.3. Isotopic ^{13}C labeled study for validating proposed mechanisms for anisole and phenol. Experiments were performed using ^{13}C labeled anisole (anisole-phenyl-$^{13}C_6$) and phenol (phenol-1-^{13}C) isotopes to further validate the major steps involved in the proposed mechanisms. For all pyrolysis runs, EI fragmentation patterns in MSD are assumed similar for both regular molecules and ^{13}C labeled isotopes. All calculations were performed after deducting the estimated overlapping ion counts of the fragments generated from H cleavage in the EI fragmentation step.

The MSD-EI spectrum for benzene produced from anisole (Fig. 5) showed a major M+ peak at m/z = 84, probably coming from the benzene ring of anisole. During the production of benzene from anisole, the probability of benzene forming exclusively from ^{13}C carbons was 70% (Fig. 5). This show that the anisole benzene ring is mostly preserved to produce benzene in the anisole conversion as illustrated in the anisole mechanism of Fig. 2. Theoretically, a perfectly scrambled

Table 3 Product selectivity for conversion of 1,4 benzoquinone, hydroquinone and catechol over zeolite (volatilizing temperature = 600 °C, catalyst bed temperature = 600 °C, reactant loading = 0.25 mg, catalyst CBV 2314, catalyst loading = 40 mg)

Feedstock	Phenol	1,4-Benzoquinone	Hydroquinone	Catechol
Benzene	34.2 ± 0.8	37.1 ± 0.1	37.4 ± 0.5	40.8 ± 0.4
Toluene	2.2 ± 0.2	9.6 ± 0.2	12.9 ± 0.8	22.3 ± 1.3
C8 aromatics[a]	0.4 ± 0.1	1.2 ± 0.1	2.2 ± 0.4	4.5 ± 0.7
Naphthalene	27.9 ± 0.6	28.2 ± 0.3	30.0 ± 1.8	16.2 ± 1.1
Biphenyl	11.7 ± 0.0	1.9 ± 1.3	0.7 ± 0.0	0.6 ± 0.3
C9 aromatics[b]	2.1 ± 0.1	2.6 ± 0.3	0.7 ± 0.2	3.5 ± 0.1
C10+ aromatics[c]	21.7 ± 0.3	6.6 ± 1.2	16.1 ± 0.0	12.1 ± 0.3

[a] C8 aromatics including xylenes and ethylbenzene. [b] C9 aromatics include indene and alkybenzenes. [c] C10+ aromatics include alkylated naphthalenes and higher polyaromatic hydrocarbons (PAHs).

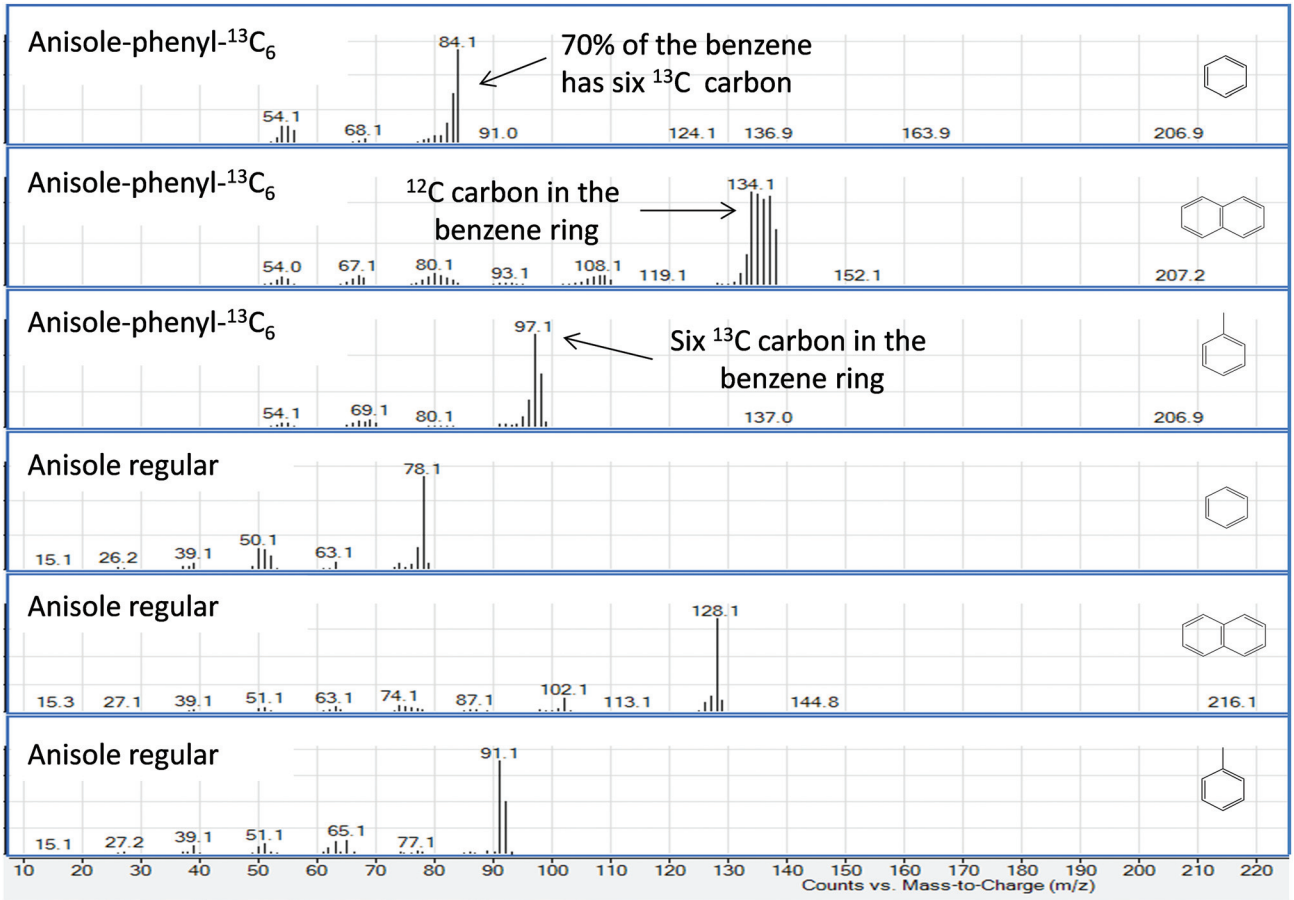

Fig. 5 MSD-EI spectra for benzene, naphthalene and toluene produced from anisole-phenyl-$^{13}C_6$ and regular anisole during catalytic pyrolysis over zeolites at 600 °C.

system of seven carbons with six ^{13}C carbons will only have a 14% probability of having all ^{13}C carbons in the benzene ring. However, for naphthalene, only 17% (m/z = 138) of the total count are formed exclusively from ^{13}C carbon atoms, indicating a contribution of the ^{12}C methoxy carbon atoms in naphthalene formation, as shown in Fig. 2. Toluene and xylene (not illustrated) produced from anisole isotope has M+ equivalent to exactly six atomic mass units higher than the corresponding ions for regular ^{12}C anisole (Fig. 5). This indicates that ^{12}C carbon in the methoxy group of anisole apparently participates in alkylation of benzene to produce the toluene and xylenes, as illustrated in the anisole mechanism (Fig. 2).

In preliminary runs with phenol isotope over zeolites, evolved phenol had only 45% of the original isotope (^{13}C position carbon in C-1) as apparent from MSD Electron Ionization (EI) patterns (see Fig. S4 in ESI† for further details). One explanation for this phenomenon could be isomerization reactions of phenol on the external surface acid sites of the zeolite catalyst. For subsequent calculations, it was assumed that only 45% of the original phenol isotope was available for secondary phenol conversion reactions, assuming phenol isomerization occur initially over the external surface of the zeolite.

Reaction of phenol isotope over zeolites show that product benzene has a main M+ peak of m/z = 79, similar to phenol-1-^{13}C benzene ring (Fig. 6). This imply that benzene is formed primarily (79%) by coupling of aryl and hydrogen radicals, as shown in the radical recombination step in the phenol mechanism (Fig. 3). Around 13.9% (m/z = 78) of the benzene is exclusively formed from ^{12}C carbons, possibly derived from the ring opening step described in the phenol mechanism of Fig. 3 (secondary benzene formation route). As indicated in Fig. 6, 8.8% of the naphthalene is exclusively formed from ^{12}C carbon atoms (m/z = 128). This naphthalene generation step should have a similar bi-radical route as illustrated in Fig. 3. If we assume all naphthalene was formed from benzene, the observed yield of 8.8% represents 98% of the theoretical maximum yield of 9.0%, calculated assuming perfect mechanism and 45% availability of original isotope (phenol-1-^{13}C) due to phenol isomerization. This value (8.8%) is 167% higher than the random naphthalene formed exclusively from ^{12}C (5.3%), calculated assuming arbitrary contributions from perfectly scrambled carbon atoms of phenol isotope molecule. These observations provide evidence that naphthalene formation on benzene ring mostly do not use C-1 carbon as it is lost as carbon monoxide similar to that for the phenol mechanism (Fig. 3).

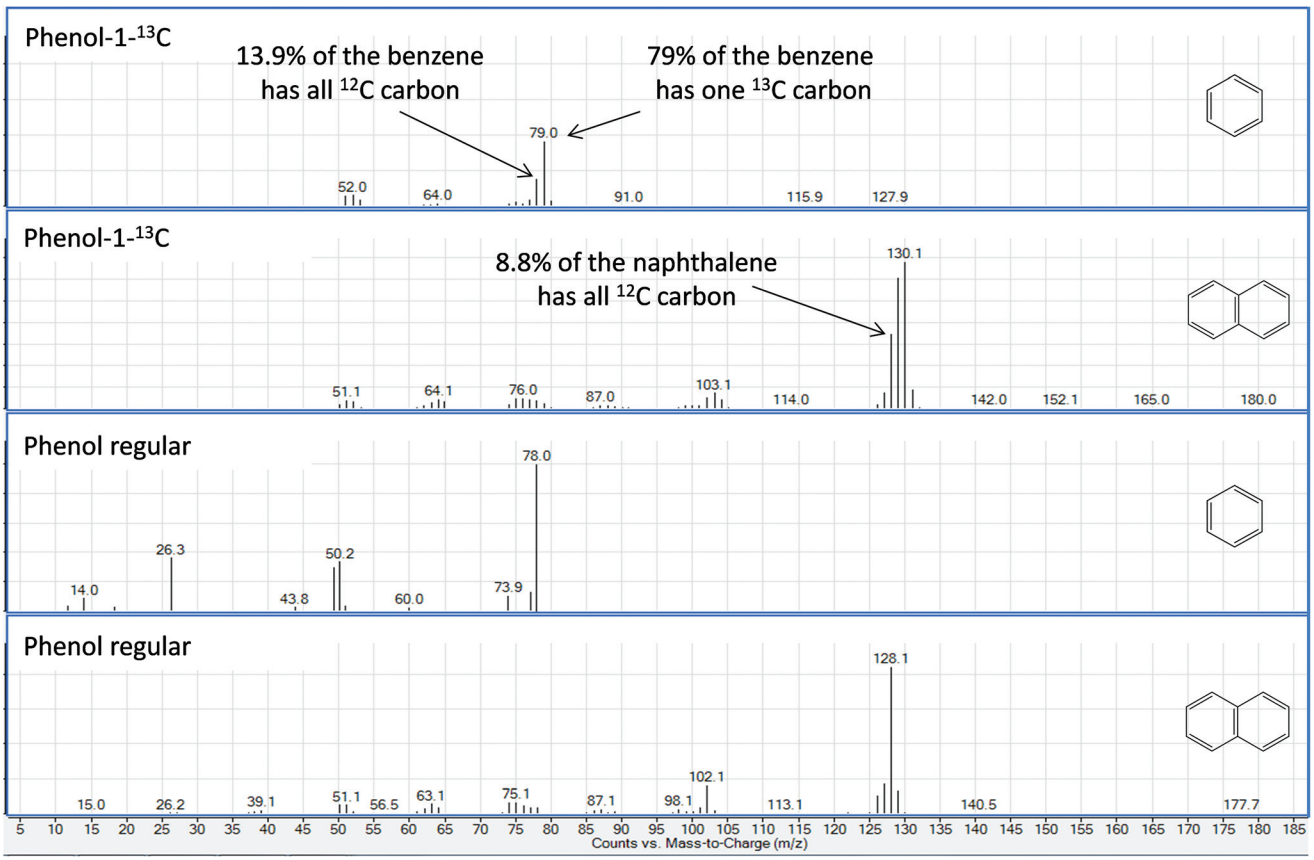

Fig. 6 MSD-EI spectra for benzene and naphthalene produced from phenol-1-^{13}C and regular phenol during catalytic pyrolysis over zeolites at 600 °C.

3.2. Understanding the conversion of phenol over zeolite in presence of water

Since water is a major constituent of most biomass, its effect on reaction mechanisms should be considered. As shown in Fig. 7, the introduction of water with the sample dramatically increased monoaromatic products and reduced PAHs, especially naphthalene and biphenyl. It is hypothesized that water increases the formation of hydrogen and hydroxyl radicals by shifting the equilibrium of the water-forming radical reaction. Hydrogen enhances saturation of double bonds in the fractionated intermediates, encouraging formation of monoaromatic compounds. Hydroxyl radicals enhance phenol ring-opening reactions while PAHs and coke generation are expected to decrease with increasing hydrogenation. For 1 : 20 phenol-to-water ratio, overall conversion to aromatic hydrocarbons increased to 43.7%. With enhanced hydrogenation, conversion *via* phenol isomer 2,4-cylohexadienone (Fig. S3 in ESI†) was also expected, which could generate more monoaromatics.

3.3. Significance of the anisole and phenol conversion mechanisms

Phenol readily polymerizes and dehydrates to char when heated even in the absence of zeolite catalyst. However, we found that in the presence of a methenium ion, the CO bond in phenol can be replaced with a carbon–carbon bond to form benzaldehyde, which readily converts to benzene over zeolite catalyst. Methenium ions generated were also identified as an alkylating agent for aromatic hydrocarbons produced inside zeolite pores. The proposed mechanism for anisole conversion over zeolites suggests that the carbon pool formed from anisole might consist of methenium ions on the acid sites of the catalyst.

The ring opening reactions proposed for the conversion of phenol provides new insight into the naphthalenes and PAHs formation that lead to excessive coke during catalytic pyrolysis. The mechanisms for both phenol and anisole conversion have routes to high molecular weight PAHs. However dehydrogenation of phenol to form naphthalene only involves the removal of two hydrogen atoms, so coke might be expected to be more readily formed from phenol than anisole, which requires the loss of eight hydrogen atoms to form naphthalene. This study also indicated the influence of strong OH bond in phenol on PAHs and coke formation.

Water has a dramatic effect on phenol conversion, completely changing product distribution, as shown in Fig. 7. Bio-oil contain large amount of water and considerable amount of phenols that could be used to produce aromatic hydrocarbons using zeolites as described in this study.

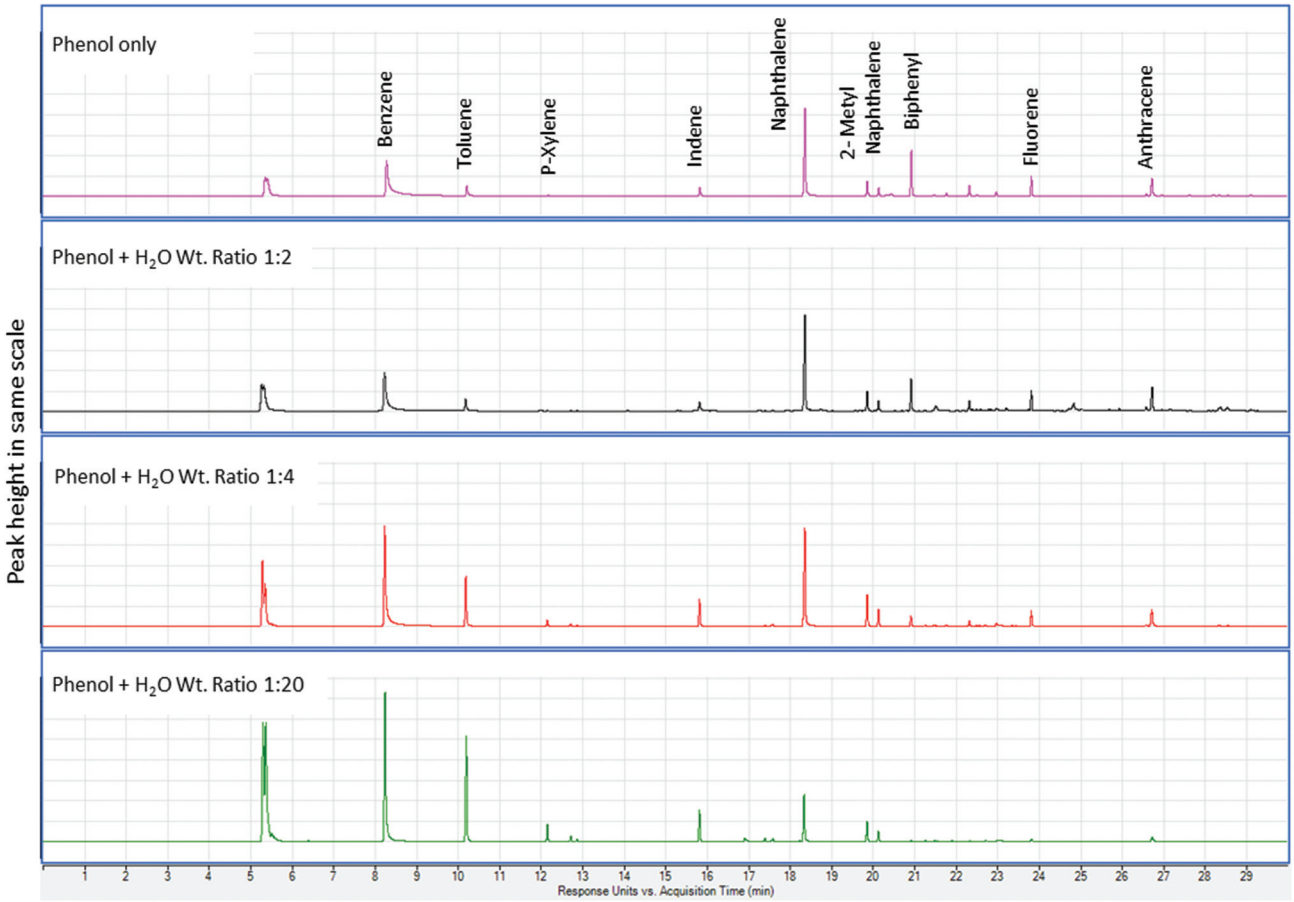

Fig. 7 Comparative GC-FID spectra showing effect of water on conversion of phenol over zeolite at 600 °C.

As a summary, study results inform us the importance of removing the phenolic hydroxyl functionalities which is a precursor for coke formation by converting them to beneficial methoxy functionality by the use of methylene donors. Basics understood from these mechanisms are expected to be useful in solving complex issues of phenolic monomers, oligomers and polymers in bio-oil and lignin.

4. Conclusion

Reaction mechanisms are proposed for the conversion of anisole and phenol over zeolites into aromatic compounds. The different product selectivities for these two phenolic reactants suggest distinctive reaction mechanisms. Anisole is thought to be converted to aromatic hydrocarbons *via* phenol and benzaldehyde intermediates, while phenol is mainly converted *via* 1,4-benzoquinone. Methenium ions and hydroxyl radicals are proposed as the most influential intermediates for anisole and phenol conversion, respectively. The proposed anisole mechanism shows methenium ions convert phenol and alkylate aromatic hydrocarbons inside zeolite pores. Phenol mechanism illustrates how intermediate bi-radicals generate polyaromatic hydrocarbons (PAHs) in zeolites. Product selectivities of major intermediates under identical reaction conditions are used to validate the mechanisms proposed for anisole and phenol. Further validation of the proposed mechanisms was carried out by using anisole and phenol with ^{13}C carbon labeled isotopes. Addition of water increased the conversion of phenol mainly to monoaromatic compounds, probably due to high temperature hydrolysis of water to hydrogen and hydroxyl radicals.

Acknowledgements

The authors would like to acknowledge financial support from the U.S. Department of Agriculture (Contract No. 2011-68005-30411). The authors would also like to thank Gayan Abeykoon, Nuwan de Silva and Umayangani Wanninayake of the Chemistry Department of Iowa State University for helpful suggestions about reaction mechanisms.

References

1 M. Guisnet and J. P. Gilson, *Zeolites for cleaner technologies*, Imperial College Press, 2002.

2 Y. T. Cheng, J. Jae, J. Shi, W. Fan and G. W. Huber, *Angew. Chem., Int. Ed.*, 2012, **51**, 1387–1390.
3 A. J. Foster, J. Jae, Y.-T. Cheng, G. W. Huber and R. F. Lobo, *Appl. Catal., A*, 2012, **423–424**, 154–161.
4 T. R. Carlson, T. P. Vispute and G. W. Huber, *ChemSusChem*, 2008, **1**, 397–400.
5 T. R. Carlson, Y. T. Cheng, J. Jae and G. W. Huber, *Energy Environ. Sci.*, 2011, **4**, 145.
6 K. Wang, J. Zhang, B. H. Shanks and R. C. Brown, *Green Chem.*, 2015, **17**, 557–564.
7 K. Wang, K. H. Kim and R. C. Brown, *Green Chem.*, 2014, **16**, 727–735.
8 K. Wang, P. A. Johnston and R. C. Brown, *Bioresour. Technol.*, 2014, **173**, 124–131.
9 B. L. S. Ivanova, B. Madani, J. P. Tessonnier, M. J. Ledoux and C. Pham-Huu, *J. Phys. Chem.*, 2007, **111**, 4368–4374.
10 X. Bai, K. H. Kim, R. C. Brown, E. Dalluge, C. Hutchinson, Y. J. Lee and D. Dalluge, *Fuel*, 2014, **128**, 170–179.
11 K. H. Kim, X. Bai and R. C. Brown, *J. Anal. Appl. Pyrolysis*, 2014, **110**, 254–263.
12 T. Kotake, H. Kawamoto and S. Saka, *J. Anal. Appl. Pyrolysis*, 2014, **105**, 309–316.
13 Z. Ma, E. Troussard and J. A. van Bokhoven, *Appl. Catal., A*, 2012, **423–424**, 130–136.
14 X. Li, L. Su, Y. Wang, Y. Yu, C. Wang, X. Li and Z. Wang, *Front. Environ. Sci. Eng.*, 2012, **6**, 295–303.
15 R. Thilakaratne, T. Brown, Y. Li, G. Hu and R. Brown, *Green Chem.*, 2014, **16**, 627–636.
16 R. Thilakaratne, M. M. Wright and R. C. Brown, *Fuel*, 2014, **128**, 104–112.
17 K. H. Kim, X. Bai and R. C. Brown, *J. Anal. Appl. Pyrolysis*, 2014, **110**, 254–263.
18 L. Zhu and J. W. Bozzelli, *J. Phys. Chem. A*, 2003, **107**, 3696–3703.
19 A. V. Friderichsen, E. J. Shin, R. J. Evans, M. R. Nimlos, D. C. Dayton and G. B. Ellison, *Fuel*, 2000, **80**, 1747–1755.
20 M. Nowakowska, O. Herbinet, A. Dufour and P.-A. Glaude, *Combust. Flame*, 2014, **161**, 1474–1488.
21 M. R. Rahimpour, A. Jahanmiri, P. Rostami, H. Taghvaei and B. C. Gates, *Energy Fuels*, 2013, **27**, 7424–7431.
22 T. Prasomsri, A. T. To, S. Crossley, W. E. Alvarez and D. E. Resasco, *Appl. Catal., B*, 2011, **106**, 204–211.
23 K. H. Kim, X. Bai, S. Cady, P. Gable and R. C. Brown, *ChemSusChem*, 2015, **8**, 894–900.
24 F. Carey, *On-Line Learning Center for Organic Chemistry*, 1992.
25 G. A. Olah, *Acc. Chem. Res.*, 1971, **4**, 240–248.
26 *The Chemistry of phenols*, ed. Z. Rapport, Wiley, 2003.
27 J. A. Berson, in *Rearrangements in Ground and Excited States: Organic Chemistry: A Series of Monographs*, 2013, vol. 1, p. 311.
28 W. Sesselmann, B. Woratschek, G. Ertl, J. Küppers and H. Haberland, *Surf. Sci.*, 1983, **130**, 245–258.
29 M. Kaltchev, D. Stacchiola, H. Molero, G. Wu, A. Blumenfeld and W. Tysoe, *Catal. Lett.*, 1999, **60**, 11–14.
30 I. M. Abdelrehim, N. A. Thornburg, J. T. Sloan, T. E. Caldwell and D. P. Land, *J. Am. Chem. Soc.*, 1995, **117**, 9509–9514.
31 R. C. Brown, *Biorenewable Resources: Engineering New Products from Agriculture*, Iowa State Press, 2003.
32 S. J. Blanksby and G. B. Ellison, *Acc. Chem. Res.*, 2003, **36**, 255–263.
33 J. Li, E. Kennedy and M. Stockenhuber, *Catal. Lett.*, 2014, **144**, 9–15.
34 W. Wang, Y. Jiang and M. Hunger, *Catal. Today*, 2006, **113**, 102–114.